Composites Part B 268 (2024) 111075

Contents lists available at ScienceDirect

Composites Part B

journal homepage: www.elsevier.com/locate/compositesb

Construction of an epoxidized, phosphorus-based poly(styrene butadiene styrene) and its application in high-performance epoxy resin

Cheng Wang [a], Siqi Huo [b,c,*], Guofeng Ye [a], Bingtao Wang [d], Zhenghong Guo [d], Qi Zhang [a], Pingan Song [b,e], Hao Wang [b,**], Zhitian Liu [a,***]

[a] Hubei Engineering Technology Research Center of Optoelectronic and New Energy Materials, School of Materials Science & Engineering, Wuhan Institute of Technology, Wuhan, 430205, China
[b] Centre for Future Materials, University of Southern Queensland, Springfield Central, 4300, Australia
[c] School of Engineering, University of Southern Queensland, Springfield Central, 4300, Australia
[d] Laboratory of Polymer Materials and Engineering, NingboTech University, Ningbo, 315100, China
[e] School of Agriculture and Environmental Science, University of Southern Queensland, Springfield Central, 4300, Australia

ARTICLE INFO

Keywords:
Poly(styrene butadiene styrene)
Epoxy resin
Mechanical properties
Fire safety
Dielectric performances

ABSTRACT

In modern industries, the demand of multifunctional, transparent epoxy resin (EP) combining superior dielectric, mechanical, and fire-safety performances is gradually increasing. However, it was difficult to realize such a performance portfolio in current research. Herein, we fabricated an epoxidized, phosphaphenanthrene-containing poly(styrene butadiene styrene) (ESD) for advanced fire-safe EP. ESD maintains the high transparency of EP and improves the UV-blocking property. 10 wt% ESD makes EP/DDM/10ESD pass a limiting oxygen index (LOI) of 36.0 % and a UL-94 V-0 rating. EP/DDM/10ESD displays improved mechanical properties because of intramolecular cavities and rigid P-based groups in ESD, as reflected by 79.2 %, 68.9 %, and 67.6 % increases in impact strength, tensile strength, and fracture toughness (K_{IC}) relative to EP/DDM. Compared with EP/DDM, EP/DDM/10ESD shows obviously-decreased dielectric constant and loss. EP/DDM/10ESD outperforms many fire-safe epoxy resins due to its superior comprehensive performances. Thus, this work delivers an effective method for developing multifunctional flame-retardant epoxy resin.

1. Introduction

EPs are widely applied in adhesives, coatings, printed circuit boards, electronic packaging, and electrical insulating substances due to high thermal and chemical stability, low cost, and excellent electrical insulation and mechanical properties [1–3]. With the development of electrical, electronic and communications industries, extremely strict performance requirements have been put forwards for polymeric materials recently [4]. Moreover, EPs are intrinsically combustible, and they tend to produce a mass of smoke in the burning process, limiting their applications in electrical and electronic fields [5,6]. Adding flame retardant is a common strategy to enhance flame retardancy, but their addition usually leads to the increased dielectric constant and loss, making the flame-retardant EPs fail to satisfy the requirements of electrical/electronic devices [7]. Meanwhile, the high brittleness is another major obstacle, which limits the high-performance applications of EPs [8,9]. Therefore, it is very necessary to design multifunctional EPs with superior mechanical properties, excellent fire safety, and low dielectric constant and loss.

To overcome the flammability issue of EPs, different kinds of flame retardants have been used in recent years [10,11]. Halogenated flame retardants (HFRs) show high efficiency, but many of them have been banned in industries due to the release of large amounts of toxic and acidic smoke during combustion [8,12]. Phosphorus-based flame retardants (PFRs) show great potential to replace HFRs because of high thermal stability and low toxicity and smoke [2,13,14]. As a typical PFR, 9,10-dihydro-9-oxo-10-phosphaphenanthrene-10-oxide (DOPO) has gained more and more attention for high reactivity and multiple fire-retardant functions [15,16]. Wang *et al.* [17] reported a DOPO derivative (DOPO-THPO) to flame retardant EPs. The as-prepared EP

* Corresponding author. Centre for Future Materials, University of Southern Queensland, Springfield Central, 4300, Australia.
** Corresponding author.
*** Corresponding author.
E-mail addresses: Siqi.Huo@unisq.edu.au, sqhuo@hotmail.com (S. Huo), hao.wang@unisq.edu.au (H. Wang), able.ztliu@wit.edu.cn (Z. Liu).

https://doi.org/10.1016/j.compositesb.2023.111075
Received 18 August 2023; Received in revised form 10 October 2023; Accepted 23 October 2023
Available online 23 October 2023

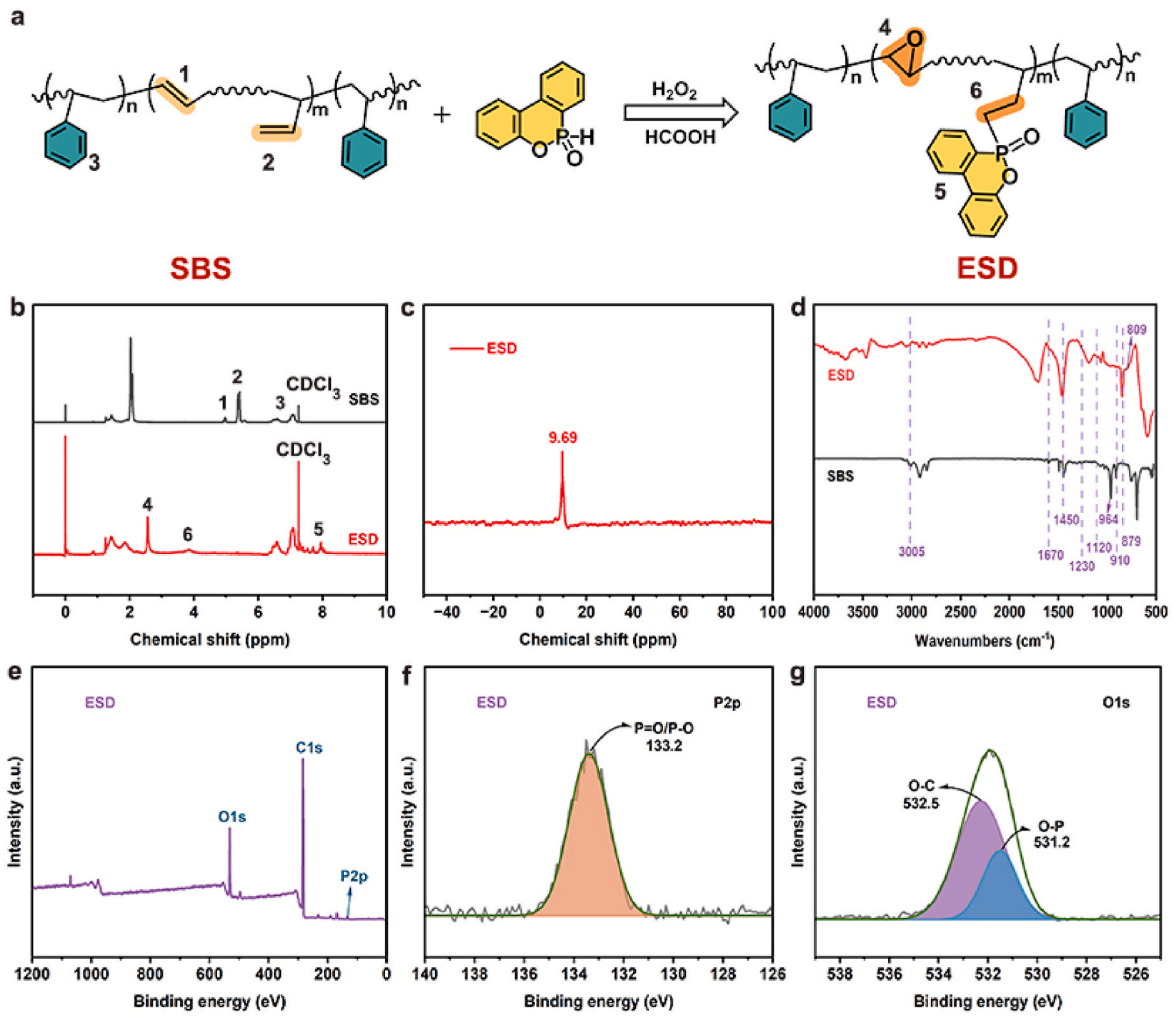

Fig. 1. (a) Synthesis of ESD, (b) ^{1}H NMR spectra of SBS and ESD, (c) ^{31}P NMR spectrum of ESD, (d) FTIR spectra of SBS and ESD, (e) XPS full-scan spectrum, and (f) P2p and (g) O1s spectra of ESD.

system with a phosphorus content of 0.33 wt% reached a LOI of 30.0 % and a UL-94 V-0 rating, indicating satisfactory flame retardancy. Jian *et al.* [18] developed a nitrogen-containing DOPO derivative (DOPO-ABZ), which was also applied in EP. Adding 7.5 wt% of DOPO-ABZ enhanced the LOI and UL-94 classification of EP to 33.5 % and V-0, with obviously reduced heat and smoke release. Unfortunately, these PFRs are rich in polar groups and suffer from plasticizing effect, and thus they tend to deteriorate the mechanical and dielectric properties of epoxy resin [19,20]. Therefore, the development of multifunctional PFRs is critical to address the trade-off between flame retardancy and mechanical/dielectric properties.

The highly cross-linked network of EPs is responsible to their poor toughness [8,21]. Introducing block copolymers is an effective method to toughen epoxy resins [22,23], which will form 'sea-island separation' structure within the EP matrix, thus contributing to the dissipation of energy under external forces [24,25]. Poly(styrene-butadiene-styrene) (SBS) is a commercial copolymer, which has the advantages of both plastic and rubber [26]. However, the unmodified SBS is incompatible with epoxy resins, making it impossible to toughen EPs directly. The epoxidation of SBS is an effective way to enhance its compatibility with EP, and some relevant works had been reported [24,26,27]. George *et al.* [24] successfully synthesized epoxidized styrene-butadiene-block-styrene (eSBS) triblock copolymers using a hydrogen peroxide/dichloroethane biphasic system. The impact strength and fracture toughness of EP/eSBS/DDM system were significantly improved compared with the unmodified system. However, the current research only focused on the toughening modification of EPs, which ignored the importance of flame retardancy and dielectric properties.

The dielectric properties of polymers mainly originate from dipole relaxation and orientation. Reducing the dipole strength of polymer is an effective way to decrease the dielectric constant and loss [28]. Introducing another polymer network in the EP can form many bound regions, thus reducing the dipole strength [29,30]. Obviously, the epoxidized SBS can form many binding areas with EP through covalent linkage, thus enhancing the dielectric properties. Therefore, combining PFR and epoxidized SBS is expected to create multifunctional flame retardants for EP.

A DOPO-containing, epoxidized SBS (ESD) was created successfully in this work for the preparation of multifunctional epoxy resins. The impacts of ESD on the thermal, optical, mechanical, dielectric, and flame-retardant performances of EP were investigated in detail. In addition, the reinforcing, toughening and fire-retardant mechanisms of ESD were studied. This work offers a reasonable design for creating multifunctional EPs with superior optical, mechanical, dielectric, and fire-retardant performances, which are of great prospect in various industries.

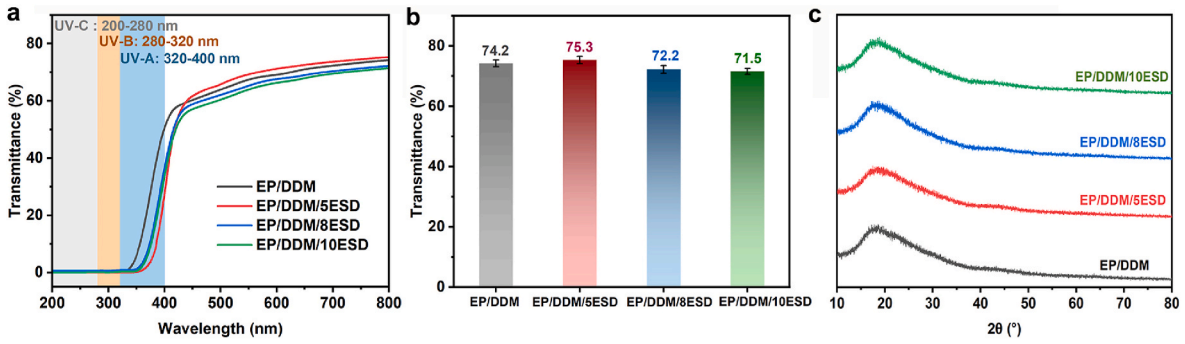

Fig. 2. (a) UV–Visible spectra, (b) light transmittances at 800 nm, and (c) XRD patterns of EP samples.

2. Experiment section

2.1. Materials

SBS with a butadiene/styrene proportion of 6/4 (126S) was obtained from Asahi Kasei Corporation (Japan). 4,4′-Methylenedianiline (DDM), DOPO and azobisisobutyronitrile (AIBN) were purchased from Energy Chemical Co., Ltd. (Shanghai, China). Xylene, hydrogen peroxide (30 % aqueous solution), formic acid (88 % aqueous solution), and methanol were provided by Sinopharm Chemical Reagent Co., Ltd. (Shanghai, China). Diglycidyl ether of bisphenol A (DGEBA, CYD-127, epoxide equivalent: 0.53 mol/100 g) was offered by Yueyang Baling Huaxing Petrochemical Co., Ltd. (Hunan, China).

2.2. Synthesis of phosphaphenanthrene-derived epoxidized SBS (ESD)

The synthesis route of ESD is shown in Fig. 1a. SBS (10.5 g), DOPO (4.8 g) and xylene (100 mL) were stirred continuously at 100 °C in a flask. The AIBN/xylene (0.0246 g/30 mL) solution was added dropwise to the flask, and then stirring for 15 h. The flask temperature was reduced to 70 °C, and formic acid (4.54 g) was introduced. After that, hydrogen peroxide (60 mL) was added slowly, and the mixture was stirred for 3 h. Anhydrous sodium carbonate was used to adjust the pH of the mixture to neutral after the flask temperature was reduced to about 30 °C. Then, the organic phase was separated and washed with plenty of H_2O to remove hydrogen peroxide. Finally, methanol was introduced to precipitate the product, and the light-yellow powder (ESD, yield: 89 %) was gained after filtration and drying under reduced pressure at 100 °C for 10 h.

2.3. Fabrication of EPs

The formula of EPs is listed in Table S1. DGEBA and ESD were stirred intensely in a flask at 70 °C for 30 min until transparent. After the addition of DDM, the mixture was stirred for 15 min and defoamed for 5 min under reduced pressure. The obtained solution was injected into the pre-heated moulds, and it was cured at 100 °C for 2 h and 150 °C for 4 h, respectively. Based on the ESD content (5, 8 and 10 wt%), the as-prepared sample was named as EP/DDM/5ESD, EP/DDM/8ESD, and EP/DDM/10ESD. The EP/DDM specimens were prepared *via* the same method without introducing ESD.

2.4. Characterizations

This is provided in the Supplementary data.

3. Results and discussion

3.1. Characterization of ESD

The structure of ESD was characterized using ^{1}H and ^{31}P nuclear magnetic resonance (NMR), Fourier transform infrared spectroscopy (FTIR) and X-ray photoelectron spectroscopy (XPS) techniques. The ^{1}H NMR spectra of SBS and ESD are shown in Fig. 1b. Regarding SBS, the chemical shifts at 7.10 and 7.05 ppm belong to the protons of phenyl group from styrene unit, and those at 4.98–5.41 ppm correspond to the olefinic protons of 1,2- and 1,4-butadiene [26]. For ESD, the signals at 4.98–5.41 ppm of olefinic protons disappear, while that corresponding to -P–CH_2– appears at 3.80 ppm, and those assigned to the protons of phenyl groups from DOPO unit appear at 7.27–7.95 ppm [19]. Moreover, only one peak appears in the ^{31}P NMR spectrum of ESD, which is located at 9.69 ppm (see Fig. 1c). All these results confirm that the DOPO molecule has been chemically linked to SBS in ESD. In addition, a signal of epoxy group appears at 2.56 ppm [26]. This proves the successful epoxidation of SBS. The NMR results indicate that the DOPO-containing epoxidized SBS (ESD) is synthesized successfully. The FTIR spectra of both SBS and ESD are presented in Fig. 1d. The characteristic bands at 964 and 910 cm^{-1} belong to C–H groups in *cis*-1,4-polybutadiene and *trans*-1,4-polybutadiene of SBS, respectively [24,26]. The peak at 3005 cm^{-1} belongs to the stretching vibration of C–H in polybutadiene [25]. The bands at 1670 and 1450 cm^{-1} correspond to –CH═CH- and aromatic ring. Regarding to ESD, the peak disappearance at 1670 cm^{-1} demonstrates that the reaction between DOPO and –CH═CH- of SBS is successful. The characteristic bands at 1120 and 1230 cm^{-1} are assigned to P-Ph and P═O groups, further indicating the existence of DOPO group in ESD [31,32]. Moreover, the stretching vibration of C–O in epoxide group is detected at around 910 cm^{-1}, and those of epoxide group are observed at 879 and 809 cm^{-1}. Thus, the FTIR result further proves the successful epoxidation and P-modification of SBS.

To further investigate the structure of ESD, the XPS measurement was performed, with the spectra shown in Fig. 1e–g and S1. As presented in Fig. 1e and Table S2, ESD contains carbon (83.23 wt%), oxygen (15.50 wt%), and phosphorus (1.27 wt%). In the C1s spectrum of ESD (see Fig. S1), there are two peaks at 284.1 and 285.4 eV, corresponding to C–C and C–O structures. In the P2p spectrum of ESD (see Fig. 1f), the peak at 133.2 eV belong to P–O/P═O of DOPO group [1,33]. Notably, two peaks appear at 532.5 and 531.2 eV in the O1s spectrum of ESD (see Fig. 1g), corresponding to O–C and O–P structures. In brief, a DOPO-containing epoxidized SBS (ESD) was synthesized in this work.

3.2. Optical performances

EPs are extensively applied as optical and electronic packaging materials due to their high transparency and cost effectiveness [34,35]. Therefore, the influences of ESD on optical performances of epoxy resin were investigated by digital camera and UV–Visible spectrophotometer (see Figs. S2 and 2). The EP/DDM film exhibits a transmittance of 74.2 % at the wavelength of 800 nm, while the transmittances of EP/DDM/ESD films are 75.3 %, 72.2 % and 71.5 %, respectively (see Fig. 2a and b). Such result reveals that ESD maintains the visible light transmittance of EP well. As presented in Fig. 2a, EP/DDM/ESD samples display better UV resistance than EP/DDM sample, as proved by the lower

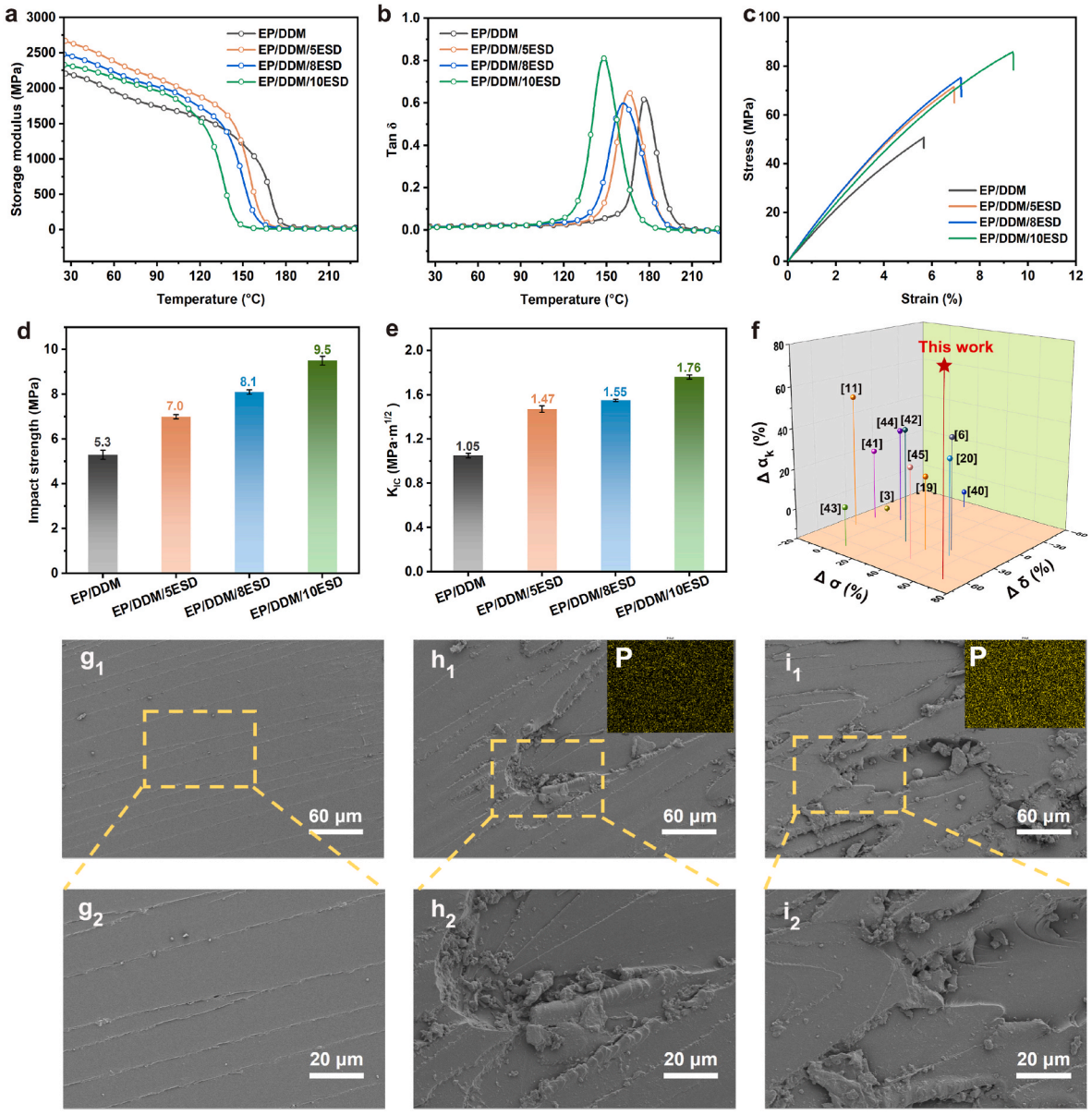

Fig. 3. (a) Storage modulus (E'), (b) tan δ, (c) tensile stress-strain curves, (d) impact strength and (e) fracture toughness (K_{IC}) values of EP samples, (f) variations in tensile strength ($\Delta\sigma$), elongation at break ($\Delta\delta$) and impact strength ($\Delta\alpha_k$) of EP/DDM/10ESD and previous flame retardant EP/DDM samples with a UL-94 V-0 rating, and SEM and P-mapping images of the fractured surfaces for (g_1, g_2) EP/DDM, (h_1, h_2) EP/DDM/8ESD, and (i_1, i_2) EP/DDM/10ESD samples obtained from the Izod notched impact tests.

transmittances between the wavelength of 200–400 nm. Obviously, the UV absorption effect of phosphaphenanthrene group in ESD is responsible to the enhanced UV resistance of EP/DDM/ESD samples [36]. The excellent compatibility of ESD and EP/DDM is the essential factor to maintain high visible light transmittance. In the digital photos of EP films (see Fig. S2), the underlying school logos are still clearly visible although covered by EP films. These results further verify that ESD effectively maintains the high transparency of EP/DDM/ESD samples and enhances the UV-shielding properties.

In accordance with previous works [37,38], the high visible light transmittance of EPs is mainly due to their non-crystalline structure. The influence of ESD on the crystalline structure of EP film was studied *via* X-ray diffraction (XRD) technique (see Fig. 2c). EP/DDM and EP/DDM/ESD samples have only one peak at $2\theta = 10°–30°$, revealing that ESD has almost no impact on the non-crystalline structure of EP. The high transparency and improved UV resistance of EP/DDM/ESD make it promising for applications in covering precision optics, semiconductor packaging, and electronic and instrument enclosures.

3.3. Mechanical properties

As presented in Fig. 3a and b, the storage modulus (E') and tan δ plots of epoxy thermosets were gained by dynamic mechanical analysis (DMA). The E' at 30 °C and glass transition temperature (T_g) are shown in Table S3. In accordance to the typical theory of rubber elasticity, the crosslink density (υ) of EP sample is calculated based on the equation: $\upsilon = E/3RT$, where R is the gas constant, and E is the E' at the temperature (T) that is 30 K higher than T_g [39]. The E' values at 30 °C of EP/DDM/ESD thermosets are higher than that of EP/DDM thermoset, demonstrating the enhanced rigidity due to the introduction of the benzene-rich ESD. Meanwhile, the E' at 30 °C gradually decreases with the increasing loading level of ESD because of the reduced υ of EP/DDM/ESD (see Table S3). The T_g values of EP/DDM/ESD samples are lower than that of EP/DDM sample (see Fig. 3b and Table S3). The T_g

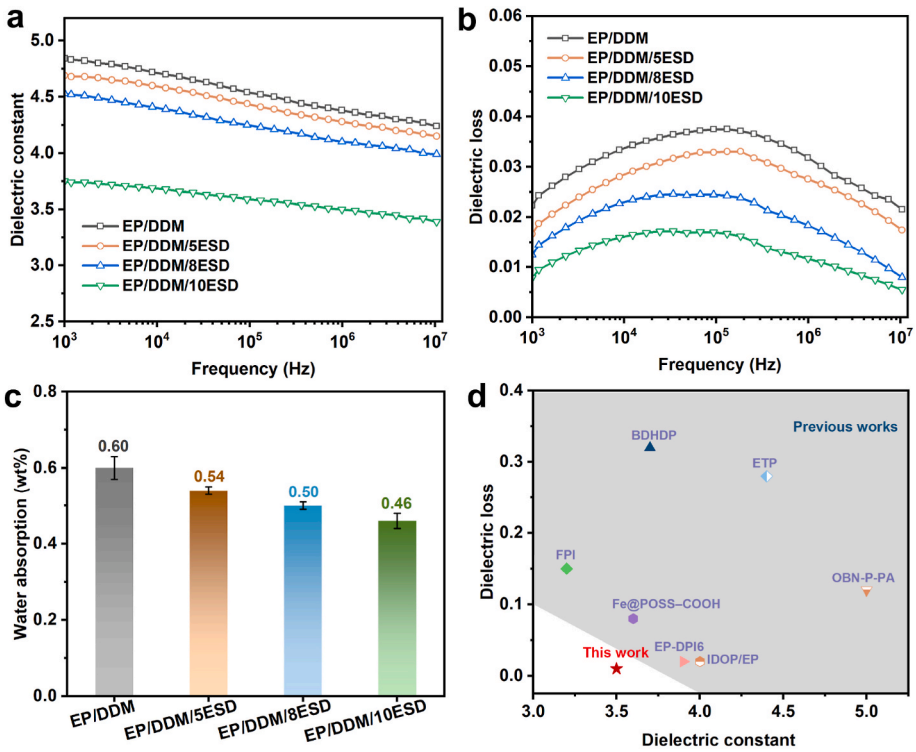

Fig. 4. The curves of (a) dielectric constant and (b) dielectric loss *vs.* frequency of EP/DDM and EP/DDM/ESD samples, (c) water absorption of EP/DDM and EP/DDM/ESD thermosets, and (d) dielectric performance comparison of EP/DDM/10ESD and previous EP thermosets with low dielectric constant/loss and UL-94 V-0 classification at 10^6 Hz.

of EP/DDM is 176.7 °C, and those of EP/DDM/5ESD, EP/DDM/8ESD and EP/DDM/10ESD are 165.6, 161.6 and 147.8 °C, respectively. Obviously, the reduction in the υ of EP/DDM/ESD is responsible for the decrease in the T_g. During curing, the epoxide group in ESD react with amino group of DDM, enabling ESD to covalently link to the EP/DDM network, bringing about the incomplete curing of DGEBA and reduced υ. In addition, ESD, as a modified SBS, forms the unique 'sea-island' phase separation structure and numerous cavities within the EP matrix [9,10], thus enhancing the polymer chain mobility and reducing the T_g of EP.

The effects of ESD on tensile properties, impact strength and fracture toughness of EP were investigated in detail (see Fig. 3b–e and Table S3). The tensile strength, elongation at break, and impact strength of virgin EP sample are 50.8 MPa, 5.7 %, and 5.3 kJ/m^2, respectively. ESD effectively enhances the mechanical properties of epoxy thermoset. For example, the tensile strength, elongation at break, and impact strength of EP/DDM/10ESD reach 85.8 MPa, 9.4 %, and 9.5 kJ/m^2, which are 68.9 %, 64.9 %, and 79.2 % higher than those of EP/DDM, respectively. Meanwhile, the K_{IC} value of EP/DDM/ESD also exhibits an increasing trend as the ESD content increases. For example, the K_{IC} of EP/DDM is 1.05 MPa m$^{1/2}$, while that of EP/DDM/10ESD is up to 1.76 MPa m$^{1/2}$, with an increase of 67.6 % (see Fig. 3e), indicative of the enhanced fracture toughness. The improved mechanical strength and toughness of EP/DDM/ESD samples are probably because the introduction of ESD endows the EP matrix with numerous rigid aromatic ring and cavities and reduced crosslinking density. In Fig. 3f and Table S4, the mechanical performances of EP/DDM/10ESD (achieving a UL-94 V-0 rating, see Section 3.7) are compared with those of previous EP/DDM systems with a UL-94 V-0 classification [3,6,11,19,20,40–45]. Obviously, EP/DDM/10ESD shows superior mechanical properties to the previously-reported EP systems, as confirmed by the higher enhancements in elongation at break and tensile and impact strengths. Such results further confirm the superior mechanical performances of EP/DDM/ESD, making it an ideal polymeric material for various high-tech applications.

To analyze the reinforcing and toughening mechanisms of ESD, the fracture surfaces of epoxy samples after the Izod notched impact tests were studied using scanning electron microscopy (SEM) and energy dispersive X-ray spectrometry (EDS) techniques. The obtained SEM and elemental mapping images are presented in Fig. 3g–i. The cross section of EP/DDM is smooth with a few linear cracks (see Fig. 3g$_1$ and g$_2$), exhibiting typical brittle fracture characteristics. On the contrary, the cross sections of both EP/DDM/8ESD and EP/DDM/10ESD are very rough, and there are many wrinkles and folds (see Fig. 3h and i). The formation of these rough and wrinkled morphologies is probably because ESD induces the plastic deformation of the substrate under external forces. In addition, the P-element mapping photos of EP/DDM/8ESD and EP/DDM/10ESD surfaces demonstrate that ESD is evenly distributed within the matrix *via* forming covalent bonds with the crosslinking network, which contributes to the improved mechanical strength and toughness.

3.4. Dielectric properties

Owing to the development of modern electrical and electronic devices, epoxy resins with low dielectric constant and loss are increasingly important [46,47]. The dielectric constant describes the charge storage capacity of material on each surface. Dielectric loss is the phenomenon of dielectric power consumption in the form of heat in an alternating electric field. The effects of ESD on dielectric properties of epoxy thermoset were evaluated (see Fig. 4a and b). All EP samples exhibit stable dielectric constants at 10^3–10^7 Hz. The dielectric constant at 10^7 Hz decreases from 4.3 for EP/DDM to 3.3 for EP/DDM/10ESD. Additionally, all EP/DDM/ESD samples present lower dielectric losses in the range of 10^3–10^7 Hz compared with EP/DDM sample, and the dielectric loss gradually decreases as the ESD content increases. For instance, EP/DDM/10ESD shows a dielectric loss of 0.005 at 10^7 Hz, with a 77.3 % decrease relative to that of EP/DDM (0.022). Moreover, the dielectric constant and loss of EP/DDM/10ESD are all lower than those of previous

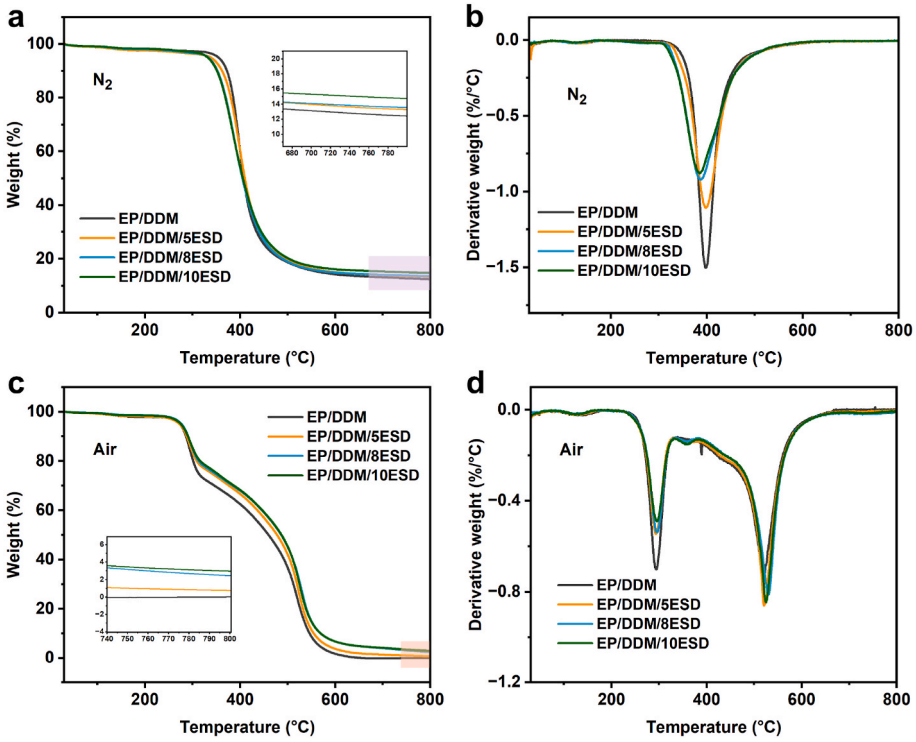

Fig. 5. (a) TG and (b) DTG curves of EP samples in N_2 condition, and (c) TG and (d) DTG curves of EP samples under air atmosphere.

low-dielectric, flame-retardant EPs at 10^6 Hz (see Fig. 4d and Table S5), indicative of superior dielectric performances [4,7,46–50]. The dielectric performances of epoxy thermosets are closely related to their free volume and polarization rate. ESD suppresses the polarizability of polar groups and limits the orientation of polymer chains under external electric fields [28]. In addition, ESD with many rigid aromatic rings as well as intramolecular cavities is chemically connected to the cross-linking network, which enlarges the free volume of epoxy thermoset. Thus, incorporating ESD reduces the dielectric constant and loss of EP.

Water has a very high dielectric constant (close to 80). Thus, the moisture has an obvious adverse effect on dielectric stability of polymers, and the water adsorption of EPs is critical for their electronic/electrical applications [46]. The water absorption of EP/DDM and EP/DDM/ESD samples was measured (see Fig. 4c). It is obvious that the introduction of ESD decreases the water absorption of EP. In particular, the water absorption of EP/DDM/10ESD reduces to 0.46 wt%, with a 23.3 % decrease compared with that of EP/DDM. The decreased water absorption of EP/DDM/ESD is mainly due to the barrier and hydrophobic effects of the evenly-dispersed ESD with abundant aromatic groups. Hence, ESD endows EP/DDM/ESD with low water absorption and dielectric constant/loss, enabling it to find ubiquitous applications in electronic/electrical fields.

3.5. Thermal stability

The thermogravimetric (TG) and derivative TG (DTG) plots of ESD and EP thermosets are shown in Figs. S3 and 5. The temperature at 5 % weight loss ($T_{5\%}$), temperature at maximum mass-loss rate (T_{max}) and char yield at 800 °C (*CY*) are listed in Table S6. The $T_{5\%}$ values of ESD in N_2 and air conditions are 249 and 242 °C, which are much higher than the curing temperature of EP/DDM (150 °C), demonstrating that ESD does not degrade during curing. Meanwhile, the *CY* values of ESD are 10.2 % and 5.0 % under nitrogen and air atmosphere, and both higher than those of SBS, demonstrating the improved char-forming ability due to the introduction of DOPO.

All epoxy samples display a one-step thermal degradation under N_2 atmosphere. The $T_{5\%}$ and T_{max1} values of EP/DDM/ESD samples are slightly decreased with the introduction of ESD (see Fig. 5a and b and Table S6) because of the catalytic degradation of DOPO group towards the EP matrix [17,51]. Meanwhile, the *CY* of EP/DDM/ESD gradually increases as the ESD addition increases. The *CY* of EP/DDM/10ESD increases from 12.4 % of EP/DDM sample to 14.7 %, with an enhancement of 18.5 %. All experimental *CY* values of EP/DDM/ESD thermosets are higher than the calculated ones, indicative of the catalytic carbonization function of ESD. Such facilitation function was also reported in many literatures on PFRs [52,53].

The thermal oxidation decomposition of EP/DDM and EP/DDM/ESD samples consists of two steps (see Fig. 5c and d). The first step is the network degradation, and the second one is the char oxidative decomposition [11]. As presented in Table S6, the $T_{5\%}$, T_{max1} and T_{max2} of all EP/DDM/ESD thermosets are close to those of EP/DDM thermoset, while the *CY* is significantly higher and increases with the increasing ESD content. Notably, the experimental *CY* values of EP/DDM/ESD samples are also much higher than the theoretical ones in air condition, further verifying that ESD promotes the charring of EP/DDM under heating. In summary, ESD effectively maintains the thermo-oxidative stability and enhances the char-formation ability of EP.

3.6. Fire safety of EP samples

The fire safety of EP/DDM and EP/DDM/ESD samples was characterized *via* LOI, UL-94 and cone calorimetry tests (see Fig. 6 and Table S7). The LOI values and UL-94 ratings of EP samples are shown in Fig. 6a. EP/DDM is highly flammable, and it shows a LOI of 26.5 % and fails the UL-94 test, demonstrating the significance of the flame-retardant modification. Adding ESD obviously increases the LOI value and UL-94 classification of EP/DDM/ESD sample. For example, EP/DDM/8ESD sample passes a UL-94 V-0 classification and a LOI of 34.5 %, demonstrating that it can be classified into self-extinguishing material. Meanwhile, the LOI of EP/DDM/10ESD reaches up to 36.0 %. Therefore, such results confirm that ESD effectively improves the flame-

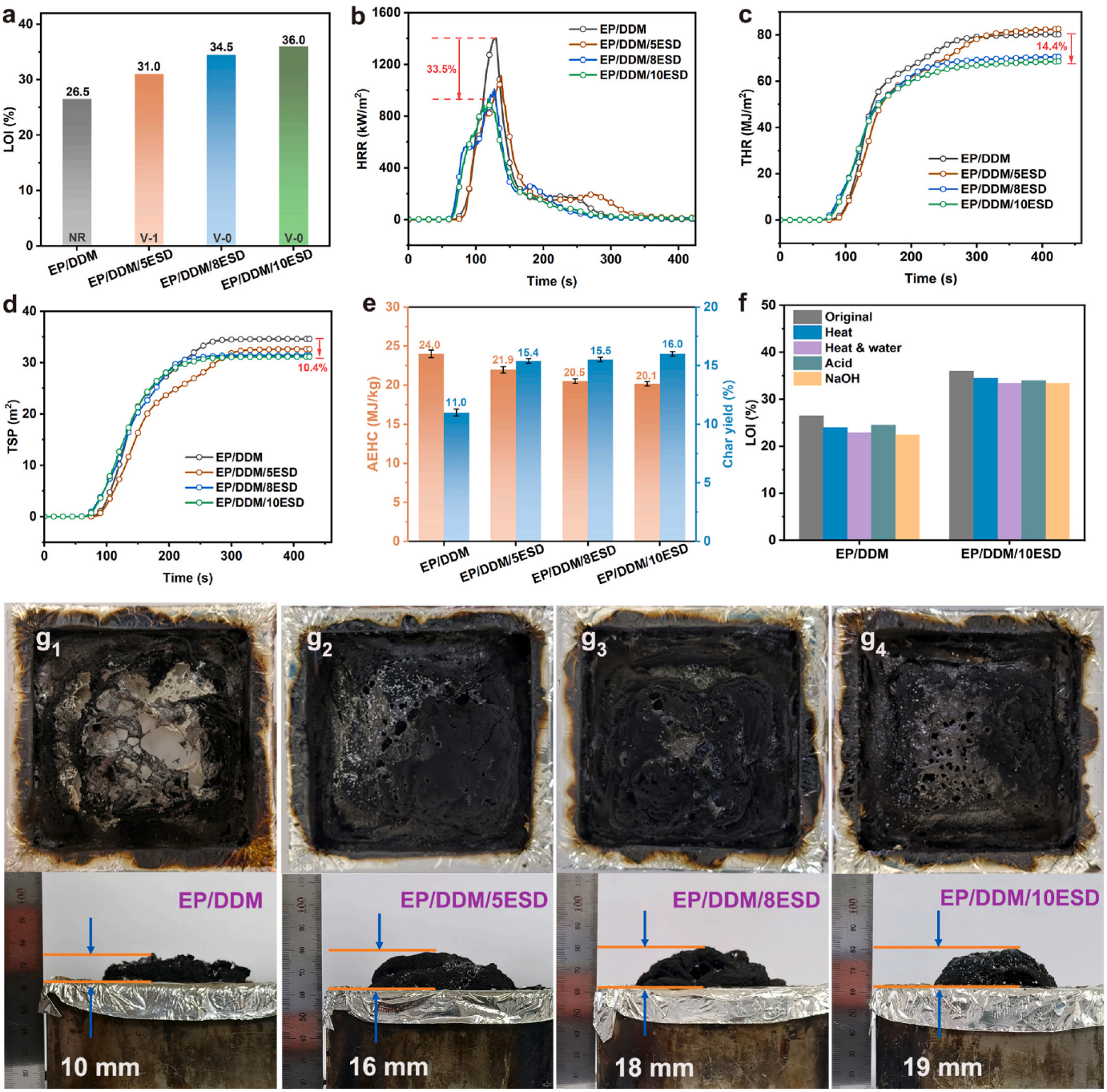

Fig. 6. (a) LOI values and UL-94 ratings, (b) heat release rate plots, (c) total heat release curves, (d) total smoke production plots, (e) average effective heat of combustion (AEHC) and char yield values of EP samples, (f) LOI values and UL-94 ratings of EP samples after different durability measurements, and top/side-view digital images of residual chars for (g_1) EP/DDM, (g_2) EP/DDM/5ESD, (g_3) EP/DDM/8ESD and (g_4) EP/DDM/10ESD after cone calorimetry tests.

retardant performances of EP/DDM.

The characteristic burning data from the cone calorimetry test are shown in Fig. 6b–e and Table S7. The time to ignition (TTI) of EP/DDM sample is 63 s, and its peak heat release rate (PHRR) and total heat release (THR) are the highest among all EP samples, reaching 1403 kW/m^2 and 80.4 MJ/m^2, respectively. The TTI of EP/DDM/ESD sample reduces with the addition of ESD because of the catalytic degradation effect of DOPO. In addition, the PHRR and THR of EP/DDM/ESD samples are much lower than those of EP/DDM sample (see Fig. 6b and c). For instance, the PHRR and THR of EP/DDM/10ESD are 933 kW/m^2 and 68.8 MJ/m^2, respectively, with 33.5 % and 14.4 % decreases compared with those of EP/DDM. Therefore, ESD is effective in suppressing the heat release of EP/DDM in the burning process. Meanwhile, the fire performance index (FPI) and fire growth rate (FIGRA) are widely used to evaluate the fire safety of material, and the FPI and FIGRA of EP/DDM and EP/DDM/ESD samples are shown in Table S7. The lower FIGRA and higher FPI demonstrate the higher fire safety [54,55]. Obviously, the EP/DDM/ESD samples have lower FIGRA and higher FPI in comparison to EP/DDM sample, further proving their higher fire safety.

In addition to intrinsic flammability, the EP/DDM sample suffers from poor smoke suppression, and its peak smoke production rate (PSPR) and total smoke production (TSP) are up to 0.47 m^2/s and 34.6 m^2, respectively (see Fig. 6d and Table S7). Introducing ESD effectively improves the smoke suppression of EP/DDM/ESD. The PSPR and TSP of

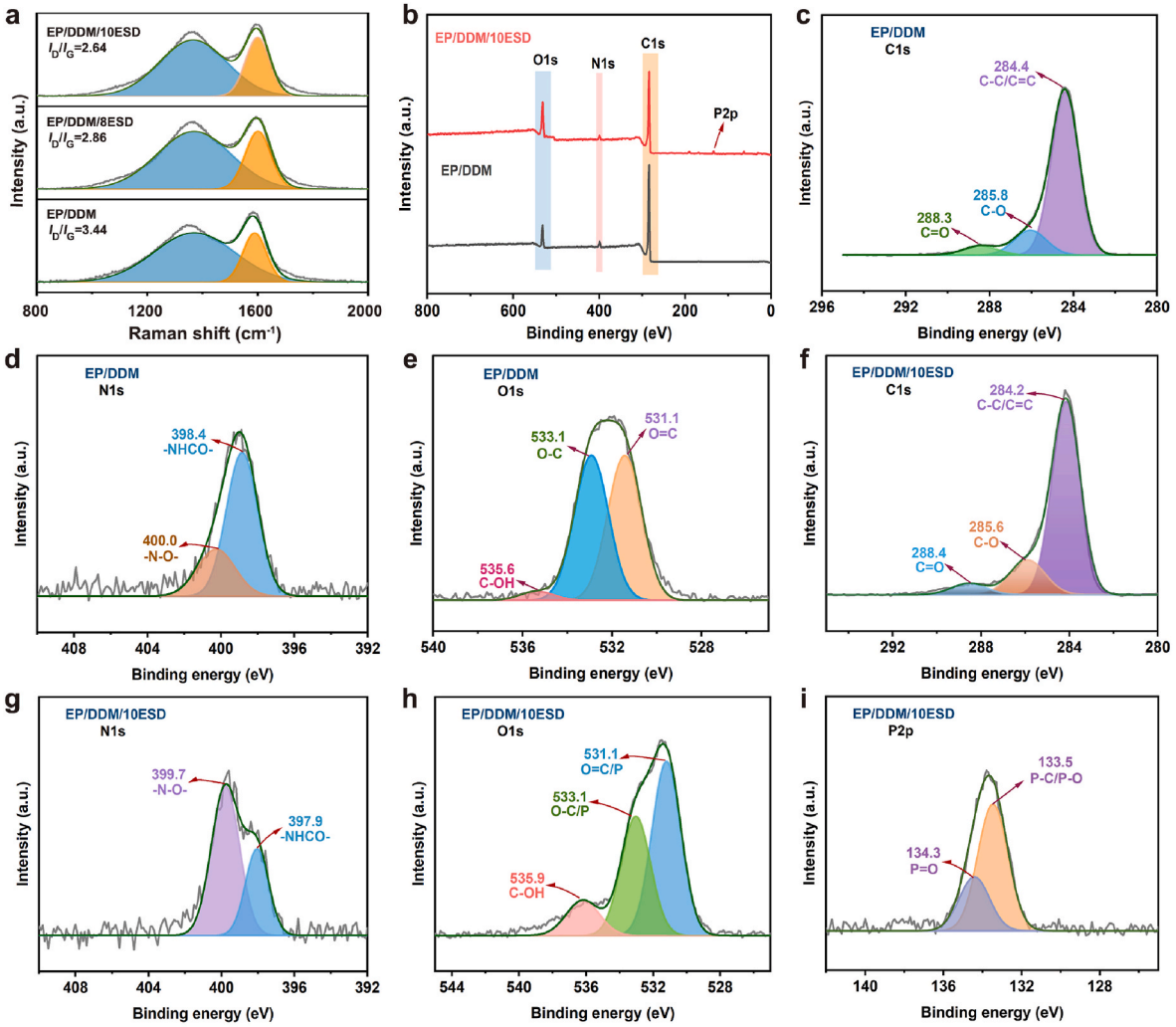

Fig. 7. (a) Raman spectra of residual chars for EP samples, (b) XPS full-scan spectra of residual chars for EP/DDM and EP/DDM/10ESD, high-resolution XPS (c) C1s, (d) N1s and (e) O1s spectra of EP/DDM char, and high-resolution XPS (f) C1s, (g) N1s, (h) O1s and (i) P2p spectra of EP/DDM/10ESD char obtained from cone calorimetry tests.

EP/DDM/10ESD are reduced by 23.4 % and 10.4 %, relative to those of EP/DDM. Furthermore, the average effective heat of combustion (AEHC) and residue char after test (RC) of EP/DDM and EP/DDM/ESD samples are presented in Fig. 6e and Table S7. According to previous works [39,56], AEHC is used to analyze the combustion degree of gaseous volatiles quantitatively. All AEHC values of EP/DDM/ESD samples are lower than that of EP/DDM sample due to the radical capturing effect of DOPO-based fragments. Additionally, all EP/DDM/ESD thermosets exhibit higher RC values than EP/DDM thermoset, which is consistent with the thermogravimetric analysis result and further proves the catalytic carbonization effect of ESD. In Fig. 6g$_1$-g$_4$, compared with the EP/DDM residue, the EP/DDM/ESD chars become denser and more intumescent with the addition of ESD, which indicates that ESD significantly enhances the char compactness and expansion height, contributing to the inhibition of heat and smoke release. Hence, the gas/condensed-phase functions of ESD are responsible for the enhanced flame retardancy and smoke suppression of EP/DDM/ES.

The fire-safe durability of polymeric materials usually determines their practical application and service life [1,19]. Therefore, the thermal/hydrothermal aging, and acid/alkali resistance tests of EP/DDM and EP/DDM/10ESD were conducted, with the results displayed in Fig. 6f and S4 and Table S8. After different durability tests, EP/DDM/10ESD still achieves a UL-94 V-0 rating and high LOI values (>33.5 %), and its weight loss rates are close to those of EP/DDM (see Fig. S4 and Table S8). Such results demonstrate that EP/DDM/10ESD features outstanding flame-retardant durability, which is probably because of the covalent linkage between ESD and cross-linked network and the macromolecular structure of ESD.

3.7. Flame-retardant mode-of-action

3.7.1. Condensed-phase action

To investigate the condensed-phase mode-of-action of ESD, the degree of graphitization and elementary content of char residues from the cone calorimetry tests were studied using Raman and XPS techniques (see Fig. 7). All Raman spectra in Fig. 7a present D and G peaks at 1364 and 1592 cm^{-1}, respectively. The D band belongs to the vibration of amorphous carbon, and the G band is assigned to the stretching vibration of graphitized carbon in the sp^2 hybridization plane. The integral area ratio of D to G bands (I_D/I_G) is inversely proportional to the graphitization degree of the carbonaceous material [57,58]. The EP/DDM char has the highest I_D/I_G value, while that of EP/DDM/ESD char gradually reduces as the ESD loading level increases. Therefore, adding ESD increases the degree of graphitization for residue, further confirming the condensed-phase effect of ESD.

The XPS spectra of EP/DDM and EP/DDM/10ESD residues are presented in Fig. 7b–i. As shown in Fig. 7b, both chars consist of carbon, oxygen, and nitrogen, while phosphorus is observed in the EP/DDM/

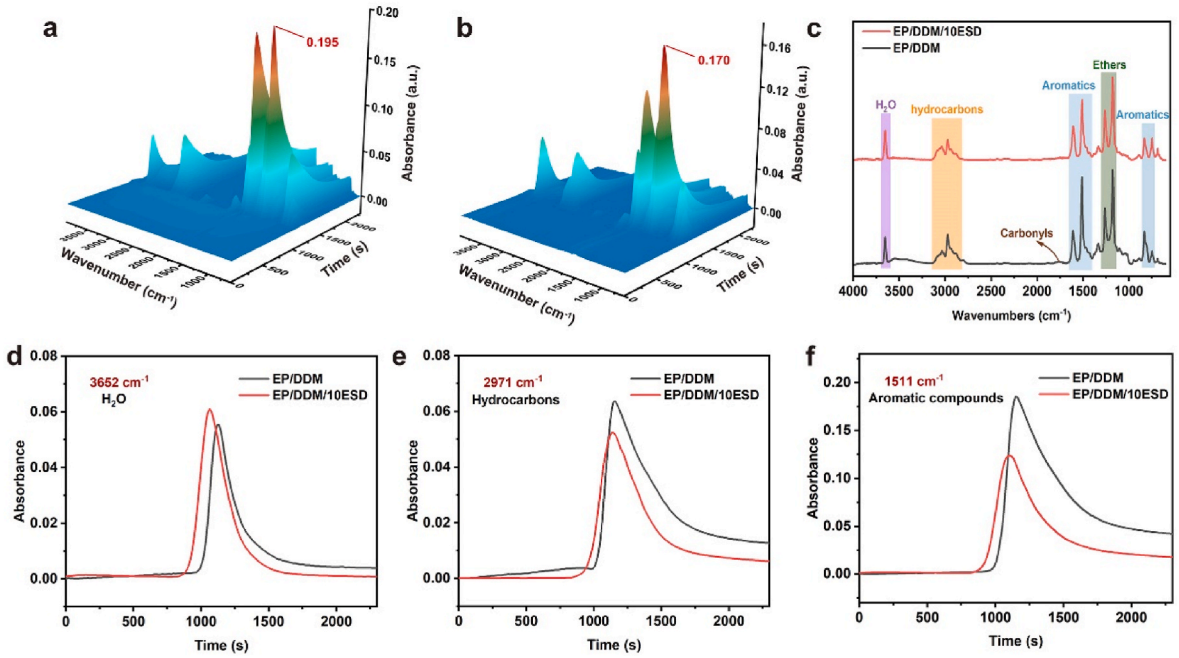

Fig. 8. 3D TG-IR spectra of pyrolysis products for (a) EP/DDM and (b) EP/DDM/10ESD samples, (c) FTIR spectra of decomposition products for EP/DDM and EP/DDM/10ESD samples at T_{max}, and the absorption *vs.* time curves of the characteristic peaks at (d) 3652, (e) 2971, and (f) 1511 cm^{-1}.

10ESD char, indicating that part of DOPO-derived groups functions in the condensed phase during combustion. The C1s, N1s and O1s spectra of EP/DDM/10ESD residue are similar to those of EP/DDM residue. In detail, the C1s spectra of both chars are deconvoluted into three peaks around 284.2, 285.6 and 288.4 eV, corresponding to C═C/C–C, C–O and C═O bonds (see Fig. 7c and f) [59,60]. The peaks around 397.9 and 399.7 eV in the N1s spectra are assigned to –NHCO– and -N-O- structures (see Fig. 7d and g) [61]. In the O1s spectrum of EP/DDM/10ESD residue, the peaks at 531.1, 533.1 and 535.9 eV belong to O═C/P, O–C/P, and C–OH bonds (see Fig. 7h) [62]. In addition, the EP/DDM/10ESD char shows P–C/P–O and P═O peaks at 133.5 and 134.3 eV in the P2p spectrum (see Fig. 7i). Such result further proves that part of phosphorus-based fragments derived from ESD are involved in charring during combustion [1,63]. Hence, the condensed-phase flame-retardant effect of ESD mainly originates from its DOPO group.

3.7.2. Gaseous-phase action

The TG-IR tests were performed on EP/DDM and EP/DDM/10ESD samples in nitrogen condition to study the effects of ESD on the decomposition gas products of EP/DDM when heated, with the relevant spectra in Fig. 8. In Fig. 8a–c, the decomposition gaseous fragments of EP/DDM and EP/DDM/10ESD are similar, mainly including water (3652 cm^{-1}), hydrocarbons (2823-3154 cm^{-1}), carbonyl derivatives (1770 cm^{-1}), aromatics compounds (1511, 1610 and 830 cm^{-1}), and ester derivatives (1176 cm^{-1}) [1,20,64]. As presented in Fig. 8d, introducing ESD increases the absorption intensity of H_2O peak because the phosphorus-containing radicals derived from ESD captures the active OH· and H· radicals to produce H_2O molecule under heating. In addition, EP/DDM/10ESD shows lower peak intensities of hydrocarbons and aromatic compounds than EP/DDM (see Fig. 8e and f), confirming that ESD retards the thermal degradation of EP/DDM and promotes the char formation at elevated temperatures.

4. Conclusions

A novel DOPO-modified epoxidized SBS (ESD) was prepared *via* a one-pot process and applied to fabricate multifunctional epoxy thermoset. The impacts of ESD on comprehensive performances of EP were studied by different experiments. The EP/DDM/ESD samples show high optical transparency and enhanced UV resistance because of the uniform dispersion of ESD and the UV absorption of its DOPO group. In addition, the EP/DDM/ESD samples show superior fire safety. The LOI and UL-94 classification of EP/DDM/10ESD can be up to 36.0 % and V-0, and its PSPR is 33.5 % lower than that of EP/DDM. EP/DDM/10ESD achieves durable flame retardancy because of the chemical connection between ESD and EP/DDM. Compared with previous flame-retardant EP/DDM systems, the EP/DDM/10ESD sample exhibits better mechanical and dielectric properties, as confirmed by 68.9 % and 79.2 % increases in tensile and impact strengths, and low dielectric constant and loss of 3.5 and 0.01 at the frequency of 10^6 Hz. Thereby, this study provides a novel design for the fabrication of multifunctional epoxy resins that are urgently needed in modern industry.

Author statement

Cheng Wang: Investigation, Data curation, Writing- Original draft. Siqi Huo: Conceptualization, Methodology, Writing - Review & Editing, Project administration. Guofeng Ye: Investigation. Bingtao Wang: Data curation. Zhenghong Guo: Data curation. Qi Zhang: Supervision. Pingan Song: Supervision. Hao Wang: Supervision. Zhitian Liu: Supervision, Funding acquisition.

Declaration of competing interest

The authors declare that they have no known competing financial interests or personal relationships that could have appeared to influence the work reported in this paper.

Data availability

Data will be made available on request.

Acknowledgements

This work was funded by the Australian Research Council Discovery Early Career Researcher Award (DE230100616), the Foundation for

Outstanding Youth Innovative Research Groups of Higher Education Institution in Hubei Province (T201706), the Foundation for Innovative Research Groups of Hubei Natural Science Foundation of China (2017CFA009), and the Major Project of Ningbo Technology Innovation 2025 (2022Z113).

Appendix A. Supplementary data

Supplementary data to this article can be found online at https://doi.org/10.1016/j.compositesb.2023.111075.

References

[1] Wang C, Huo S, Ye G, Song P, Wang H, Liu Z. A P/Si-containing polyethylenimine curing agent towards transparent, durable fire-safe, mechanically-robust and tough epoxy resins. Chem Eng J 2023;451:138768.
[2] Huo S, Song P, Yu B, Ran S, Chevali V, Liu L, et al. Phosphorus-containing flame retardant epoxy thermosets: recent advances and future perspectives. Prog Polym Sci 2021;114:101366.
[3] Shi Y, Fu T, Xu Y, Li D, Wang X, Wang Y. Novel phosphorus-containing halogen-free ionic liquid toward fire safety epoxy resin with well-balanced comprehensive performance. Chem Eng J 2018;354:208–19.
[4] Liu X, Xiao Y, Luo X, Liu B, Guo D, Chen L, et al. Flame-Retardant multifunctional epoxy resin with high performances. Chem Eng J 2022;427:132031.
[5] Wang Y, Han S, Hu X, Li W, Na B, Xie C, et al. Benefiting from the multiple effects of ferrocene and cyclotriphosphazene bi-based hierarchical layered nanosheets towards improving fire safety and mechanical properties of epoxy resin. Compos Part B Eng 2023;264:110914.
[6] Ma C, Qiu S, Yu B, Wang J, Wang C, Zeng W, et al. Economical and environment-friendly synthesis of a novel hyperbranched poly(aminomethylphosphine oxide-amine) as co-curing agent for simultaneous improvement of fire safety, glass transition temperature and toughness of epoxy resins. Chem Eng J 2017;322:618–31.
[7] Liu X, Zhou J, Wu M, Liu S, Zhao J. Design and synthesis of anhydride-terminated imide oligomer containing phosphorus and fluorine for high-performance flame-retarded epoxy resins. Chem Eng J 2023;461:142063.
[8] Qiu Y, Qian L, Feng H, Jin S, Hao J. Toughening effect and flame-retardant behaviors of phosphaphenanthrene/phenylsiloxane bigroup macromolecules in epoxy thermoset. Macromolecules 2018;51(23):9992–10002.
[9] Mi X, Liang N, Xu H, Wu J, Jiang Y, Nie B, et al. Toughness and its mechanisms in epoxy resins. Prog Mater Sci 2022;130:100977.
[10] Xu B, Zhang Q, Zhou H, Qian L, Zhao S. Small change, big impact: simply changing the substitute on Si atom towards significant improvement of flame retardancy and toughness of epoxy resins. Compos Part B Eng 2023;263:110832.
[11] Huo S, Zhou Z, Jiang J, Sai T, Ran S, Fang Z, et al. Flame-retardant, transparent, mechanically-strong and tough epoxy resin enabled by high-efficiency multifunctional boron-based polyphosphonamide. Chem Eng J 2022;427:131578.
[12] Shao Z, Yue W, Piao M, Ma J, Lv X, Wang D, et al. An excellent intrinsic transparent epoxy resin with high flame retardancy: synthesis, characterization, and properties. Macromol Mater Eng 2019;304(10):1900254.
[13] Yang S, Zhang Q, Hu Y. Synthesis of a novel flame retardant containing phosphorus, nitrogen and boron and its application in flame-retardant epoxy resin. Polym Degrad Stabil 2016;133:358–66.
[14] Huo S, Wang J, Yang S, Zhang B, Tang Y. A phosphorus-containing phenolic derivative and its application in benzoxazine resins: curing behavior, thermal, and flammability properties. J Appl Polym Sci 2016;133(19):43403.
[15] Zhang A, Zhang J, Liu L, Dai J, Lu X, Huo S, et al. Engineering phosphorus-containing lignin for epoxy biocomposites with enhanced thermal stability, fire retardancy and mechanical properties. J Mater Sci Technol 2023;167:82–93.
[16] Wen X, Liu Z, Li Z, Zhang J, Wang D, Szymanska K, et al. Constructing multifunctional nanofiller with reactive interface in PLA/CB-g-DOPO composites for simultaneously improving flame retardancy, electrical conductivity and mechanical properties. Compos Sci Technol 2020;188:107988.
[17] Wang J, Ma C, Wang P, Qiu S, Cai W, Hu Y. Ultra-low phosphorus loading to achieve the superior flame retardancy of epoxy resin. Polym Degrad Stabil 2018;149:119–28.
[18] Jian R, Wang P, Duan W, Wang J, Zheng X, Weng J. Synthesis of a novel P/N/S-containing flame retardant and its application in epoxy resin: thermal property, flame retardance, and pyrolysis behavior. Ind Eng Chem Res 2016;55(44):11520–7.
[19] Ye G, Huo S, Wang C, Song P, Fang Z, Wang H, et al. Durable flame-retardant, strong and tough epoxy resins with well-preserved thermal and optical properties via introducing a bio-based, phosphorus-phosphorus, hyperbranched oligomer. Polym Degrad Stabil 2023;207:110235.
[20] Ye G, Huo S, Wang C, Shi Q, Yu L, Liu Z, et al. A novel hyperbranched phosphorus-boron polymer for transparent, flame-retardant, smoke-suppressive, robust yet tough epoxy resins. Compos Part B Eng 2021;227:109395.
[21] Ou M, Lian R, Li R, Cui J, Guan H, Liu L, et al. Solvent-free synthesis of a hyperbranched polyphosphoramide cocuring agent and its application in fire-safe, mechanically strong, and tough epoxy resin. ACS Appl Polym Mater 2023;5(8):6504–15.
[22] Kim J, Wang V, Kim K. Block copolymers composed of main-chain cyclic polymers: morphology transition and covalent stabilization of self-assembled nanostructures via intra- and interchain cyclization of styrene-co-isoprene blocks. Macromolecules 2020;53(24):10725–33.
[23] Liu Y, Tang Z, Chen Y, Zhang C, Guo B. Engineering of β-hydroxyl esters into elastomer–nanoparticle interface toward malleable, robust, and reprocessable vitrimer composites. ACS Appl Mater Interfaces 2018;10(3):2992–3001.
[24] George S, Puglia D, Kenny J, Causin V, Parameswaranpillai J, Thomas S. Morphological and mechanical characterization of nanostructured thermosets from epoxy and styrene-block-butadiene-block-styrene triblock copolymer. Ind Eng Chem Res 2013;52(26):9121–9.
[25] George S, Puglia D, Kenny J, Parameswaranpillai J, Thomas S. Reaction-induced phase separation and thermomechanical properties in epoxidized styrene-block-butadiene-block-styrene triblock copolymer modified epoxy/DDM system. Ind Eng Chem Res 2014;53(17):6941–50.
[26] Jiang Y, Zhao R, Xi Z, Cai J, Yuan Z, Zhang J, et al. Improving toughness of epoxy asphalt binder with reactive epoxidized SBS. Mater Struct 2021;54(4):145.
[27] Rebizant V, Venet A, Tournilhac F, Girard-Reydet E, Navarro C, Pascault J, et al. Chemistry and mechanical properties of epoxy-based thermosets reinforced by reactive and nonreactive SBMX block copolymers. Macromolecules 2004;37(21):8017–27.
[28] Fu F, Zhou X, Shen M, Wang D, Xu X, Shang S, et al. Preparation of hydrophobic low-k epoxy resins with high adhesion using a benzocyclobutene-rosin modifier. ACS Sustain Chem Eng 2023;11(15):5973–85.
[29] Song N, Shi K, Yu H, Yao H, Ma T, Zhu S, et al. Decreasing the dielectric constant and water uptake of co-polyimide films by introducing hydrophobic cross-linked networks. Eur Polym J 2018;101:105–12.
[30] Song N, Yao H, Ma T, Wang T, Shi K, Tian Y, et al. Decreasing the dielectric constant and water uptake by introducing hydrophobic cross-linked networks into co-polyimide films. Appl Surf Sci 2019;480:990–7.
[31] Zhang Q, Yang S, Wang J, Cheng J, Zhang Q, Ding G, et al. A DOPO based reactive flame retardant constructed by multiple heteroaromatic groups and its application on epoxy resin: curing behavior, thermal degradation and flame retardancy. Polym Degrad Stabil 2019;167:10–20.
[32] Shi Y, Yu B, Zheng Y, Yang J, Duan Z, Hu Y. Design of reduced graphene oxide decorated with DOPO-phosphanomidate for enhanced fire safety of epoxy resin. J Colloid Interface Sci 2018;521:160–71.
[33] Wang D, Ge X, Wang Y, Wang C, Qu M, Zhou Q. A novel phosphorus-containing poly(ethylene terephthalate) nanocomposite with both flame retardancy and anti-dripping effects. Macromol Mater Eng 2006;291(6):638–45.
[34] Ai Y, Pang F, Xu Y, Jian R. Multifunctional phosphorus-containing triazolyl amine toward self-intumescent flame-retardant and mechanically strong epoxy resin with high transparency. Ind Eng Chem Res 2020;59(26):11918–29.
[35] Xing W, Song L, Jie G, Lv X, Wang X, Hu Y. Synthesis and thermal behavior of a novel UV-curable transparent flame retardant film and phosphorus-nitrogen synergism of flame retardancy. Polym Adv Technol 2011;22(12):2123–9.
[36] Yu Y, Zhang Y, Xi L, Zhao Z, Huo S, Huang G, et al. Interface nanoengineering of a core-shell structured biobased fire retardant for fire-retarding polylactide with enhanced toughness and UV protection. J Clean Prod 2022;336:130372.
[37] Ye X, Zhang W, Yang R, He J, Li J, Zhao F. Facile synthesis of lithium containing polyhedral oligomeric phenyl silsesquioxane and its superior performance in transparency, smoke suppression and flame retardancy of epoxy resin. Compos Sci Technol 2020;189:108004.
[38] Zhang Y, Liu R, Yu R, Yang K, Guo L, Yan H. Phosphorus-free hyperbranched polyborate flame retardant: ultra-high strength and toughness, reduced fire hazards and unexpected transparency for epoxy resin. Compos Part B Eng 2022;242:110101.
[39] Huo S, Yang S, Wang J, Cheng J, Zhang Q, Hu Y, et al. A liquid phosphorus-containing imidazole derivative as flame-retardant curing agent for epoxy resin with enhanced thermal latency, mechanical, and flame-retardant performances. J Hazard Mater 2020;386:121984.
[40] Ai Y, Xia L, Pang F, Xu Y, Zhao H, Jian R. Mechanically strong and flame-retardant epoxy resins with anti-corrosion performance. Compos Part B Eng 2020;193:108019.
[41] Wang W, Liu Y, Wen H, Wang Q. Synthesis of a hyperbranched polyamide charring agent and its flame-retarding and toughening behavior in epoxy resin. Polym Degrad Stabil 2021;184:109479.
[42] Sun J, Qian L, Li J. Toughening and strengthening epoxy resin with flame retardant molecular structure based on tyrosine. Polymer 2021;230:124045.
[43] Guo W, Wang X, Huang J, Mu X, Cai W, Song L, et al. Phosphorylated cardanol-formaldehyde oligomers as flame-retardant and toughening agents for epoxy thermosets. Chem Eng J 2021;423:130192.
[44] Ma C, Qiu S, Wang J, Sheng H, Zhang Y, Hu W, et al. Facile synthesis of a novel hyperbranched poly(urethane-phosphine oxide) as an effective modifier for epoxy resin. Polym Degrad Stabil 2018;154:157–69.
[45] Shi Q, Huo S, Wang C, Ye G, Yu L, Fang Z, et al. A phosphorus/silicon-based, hyperbranched polymer for high-performance, fire-safe, transparent epoxy resins. Polym Degrad Stabil 2022;203:110065.
[46] Xu Y, Chen L, Rao W, Qi M, Guo D, Liao W, et al. Latent curing epoxy system with excellent thermal stability, flame retardance and dielectric property. Chem Eng J 2018;347:223–32.
[47] Zhang W, Zhang W, Pan Y, Yang R. Facile synthesis of transition metal containing polyhedral oligomeric silsesquioxane complexes with mesoporous structures and their applications in reducing fire hazards, enhancing mechanical and dielectric properties of epoxy composites. J Hazard Mater 2021;401:123439.

[48] Yu M, Zhang T, Li J, Tan J, Zhu X. Enhancing toughness, flame retardant, hydrophobic and dielectric properties of epoxy resin by incorporating multifunctional additive containing phosphorus/silicon. Mater Des 2023;225:111529.
[49] Huo S, Sai T, Ran S, Guo Z, Fang Z, Song P, et al. A hyperbranched P/N/B-containing oligomer as multifunctional flame retardant for epoxy resins. Compos Part B Eng 2022;234:109701.
[50] Feng T, Cui J, Wang Y, Piao J, Wang Y, Ren J, et al. Self-assembly strategy to obtain phytic acid doped OBN hybrids for enhancing fire safety of epoxy resin with lower dielectric loss. Compos Commun 2022;35:101319.
[51] Huo S, Wang J, Yang S, Cai H, Zhang B, Chen X, et al. Synergistic effect between a novel triazine-based flame retardant and DOPO/HPCP on epoxy resin. Polym Adv Technol 2018;29(11):2774–83.
[52] Pourchet S, Sonnier R, Ben-Abdelkader M, Gaillard Y, Ruiz Q, Placet V, et al. New reactive isoeugenol based phosphate flame retardant: toward green epoxy resins. ACS Sustain Chem Eng 2019;7(16):14074–88.
[53] Lou G, Ma Z, Dai J, Bai Z, Fu S, Huo S, et al. Fully biobased surface-functionalized microcrystalline cellulose via green self-assembly toward fire-retardant, strong, and tough epoxy biocomposites. ACS Sustain Chem Eng 2021;9(40):13595–605.
[54] Zhou Y, Chu F, Yang W, Qiu S, Hu Y. Innovative design of hierarchical cobalt-based borate functionalized black phosphorus structure with petal-like wrinkle: enhancing the fire safety and mechanical properties of epoxy resin. Compos Part B Eng 2022;238:109886.
[55] Monti M, Camino G. Thermal and combustion behavior of polyethersulfone-boehmite nanocomposites. Polym Degrad Stabil 2013;98(9):1838–46.
[56] Gao B, Shi T, Yang X, Zhang S. Online formation of epoxy resin multi-hierarchical char layer to improve mass and heat barrier performance via designable "heterogeneous char-forming agent". Compos Part B Eng 2022;246:110145.
[57] Qiu X, Wan X, Wang Z, Li Z, Li J, Li X, et al. A simple and universal strategy for construction and application of silica-based flame-retardant nanostructure. Compos Part B Eng 2022;238:109887.
[58] Qiu S, Zhou Y, Zhou X, Zhang T, Wang C, Yuen R, et al. Air-stable polyphosphazene-functionalized few-layer black phosphorene for flame retardancy of epoxy resins. Small 2019;15(10):e1805175.
[59] Hu X, Yang H, Jiang Y, He H, Liu H, Huang H, et al. Facile synthesis of a novel transparent hyperbranched phosphorous/nitrogen-containing flame retardant and its application in reducing the fire hazard of epoxy resin. J Hazard Mater 2019;379:120793.
[60] Yang G, Wu W, Wang Y, Jiao Y, Lu L, Qu H, et al. Synthesis of a novel phosphazene-based flame retardant with active amine groups and its application in reducing the fire hazard of Epoxy Resin. J Hazard Mater 2019;366:78–87.
[61] Tan Y, Shao Z, Chen X, Long J, Chen L, Wang Y. Novel multifunctional organic-inorganic hybrid curing agent with high flame-retardant efficiency for epoxy resin. ACS Appl Mater Interfaces 2015;7(32):17919–28.
[62] Ye G, Huo S, Wang C, Shi Q, Liu Z, Wang H. One-step and green synthesis of a bio-based high-efficiency flame retardant for poly (lactic acid). Polym Degrad Stabil 2021;192:109696.
[63] Zhu M, Ma Z, Liu L, Zhang J, Huo S, Song P. Recent advances in fire-retardant rigid polyurethane foam. J Mater Sci Technol 2022;112:315–28.
[64] He L, Chen T, Wang T, Zhao H, Deng J, Li T, et al. Extra strong Cu^{2+}-doped intumescent char to protect epoxy resin against fire. Compos Part B Eng 2023;253:110539.